Nonlinear optical tuning of a two-dimensional silicon photonic crystal

H. W. Tan and H. M. van Driel
Department of Physics, University of Toronto, 60 St. George Street, Toronto, Ontario M5S1A7, Canada

S. L. Schweizer and R. B. Wehrspohn
Nanophotonics Materials Group, Department of Physics, University of Paderborn, 33095 Paderborn, Germany

U. Gösele
Max-Planck-Institute for Microstructure Physics, Weinberg 2, D-06120 Halle, Germany
(Received 30 October 2003; revised manuscript received 1 June 2004; published 8 November 2004)

We use the real (Kerr) and imaginary (two photon absorption) parts of a third order optical nonlinearity to tune the long (1.6 μm) and short wavelength (1.3 μm) band edges of a stop gap in a two-dimensional silicon photonic crystal. From pump-probe reflectivity experiments using 130 fs pulses, we observe that a 2 μm pulse induces optical tuning of the 1.3 μm edge via the Kerr effect whereas a 1.76 μm pulse induces tuning of the 1.6 μm band edge via both Kerr and Drude effects with the latter related to two-photon induced generation of free carriers with a lifetime of $\sim$900 ps.

DOI: 10.1103/PhysRevB.70.205110 PACS number(s): 42.70.Qs, 42.65.Hw, 42.65.Re

I. INTRODUCTION

Photonic crystals (PC) have unusual dispersion properties that strongly influence the propagation characteristics of light beams. However, while linear optical properties of PCs have received considerable attention, nonlinear properties are not nearly as well understood, including the extent to which nonlinear effects can be used to tune PC optical properties quickly.[1–8] In earlier work within our group,[6] linear optics, in particular single photon absorption by 800 nm, 150 fs pulses, was used to inject high carrier densities which tuned the mode frequencies of a two-dimensional (2D) photonic crystal through Drude-induced changes to the linear optical susceptibility; time-resolved frequency shifts of a Bragg gap up to 29 nm were observed. Although pulse-width limited turn-on times were observed, the recovery time was limited by carrier lifetime ($\gg$100 ps). In general, overall pulse-width limited response can only be achieved using nonresonant, nonlinear induced changes to material optical properties such as the optical Kerr effect (a third order nonlinearity) or the optical Stark effect which has been employed by Shimizu *et al.*[9] in a multicomposite 1D system. There has previously been a suggestion of Kerr-induced reflectivity changes[4,5] for PCs, but the limited data is insufficient to confirm this, or permit detailed analysis.

Here, using 130 fs pump pulses, we clearly demonstrate tuning of a 2D silicon PC using a Kerr nonlinearity. Because silicon has an indirect band gap of 1.1 eV (equivalent to $\lambda = 1.1$ μm) at 295 K and a direct gap at a relatively high energy of 3.5 eV ($\lambda = 355$ nm), relatively weak phonon assisted linear or two-photon absorption occurs across the visible and near infrared; there may then be an advantage to considering nonlinear effects in PCs made from this semiconductor. In particular we show that the short wavelength edge (1.3 μm) of a photonic band gap can be redshifted via the Kerr effect with a pump beam at 2.0 μm. For a pump wavelength of 1.76 μm and probe wavelength of 1.6 μm (the long wavelength edge of the same gap) a redshift also occurs via a Kerr effect. However at high pump intensities, generation of free carriers from two-photon absorption (2PA) becomes apparent, leading to a blueshift of the photonic band edge via a Drude contribution to the linear dielectric constant.

II. EXPERIMENTAL DETAILS

The experimental results were obtained with a parametric generator pumped by a 250 kHz repetition rate Ti-sapphire oscillator/regenerative amplifier which produces 130 fs pulses at 800 nm at an average power of 1.1 W.[10] The signal pulse from the parametric generator is tunable from 1.2 to 1.6 μm and the idler pulse is tunable from 2.1 to 1.6 μm.

The 2D silicon PC sample has a triangular lattice arrangement of 560 nm diameter, 96 μm deep air holes with a pitch, a, equal to 700 nm. Figure 1(a) shows a real space view of the sample while Fig. 1(b) illustrates the photonic band structure for the Γ-M direction, which is normal to a face of the PC. Of particular interest is the third stop gap for E-polarized (E-field parallel to the pore axis) light. Lying between 1.3 and 1.6 μm, this gap falls between two dielectric bands that are sensitive to changes in the silicon refractive index. Our purpose is to optically induce changes to the two edges with idler pulses from the parametric generator and probe these changes via time-resolved reflectivity of the signal pulses. Note that, because of the link between the signal and idler wavelengths, different pump wavelengths (2.0 μm for a 1.3 μm probe; 1.76 μm for a 1.6 μm probe) must be used when the probe wavelength is changed. However, as will be shown in what follows, small changes in the pump wavelength can lead to significant changes in the induced optical processes.

For the time-resolved reflectivity geometry, as indicated in Fig. 1(a), pump pulses polarized along the Γ-M direction are focused to a spot size of 25 μm on the top surface of the PC near a crystal face and propagate along the direction (z) of the pore axis. An E-polarized probe beam focused to a

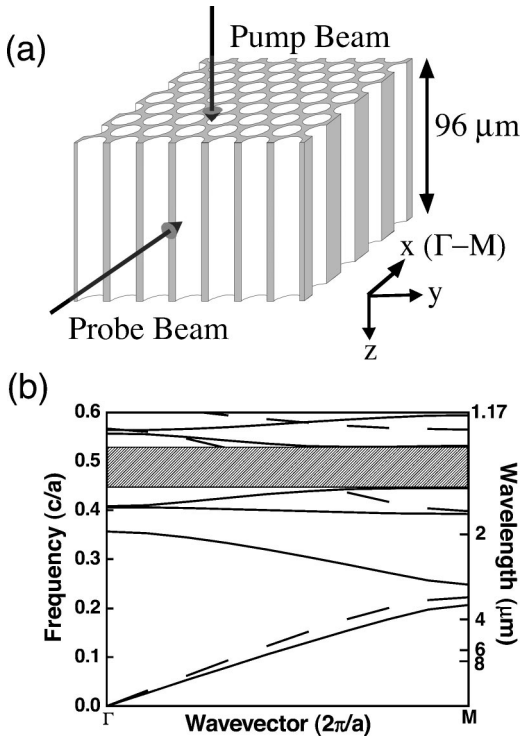

FIG. 1. (a) The 2D Si photonic crystal showing pump-probe beam geometry. The probe beam is incident along the Γ-*M* direction. (b) Band structure of the photonic crystal for the Γ-*M* direction. The solid and dashed lines correspond to *E* and *H* polarized light, respectively.

spot size of 13 μm is incident normal to the face of the PC approximately 60 μm below the entry point of the pump beam. The reflected probe beam is passed through a 0.25 mm monochromator and detected by a cooled germanium detector. The pump-probe beam geometry ensures that a reasonably uniform excitation region is probed and is also necessary to avoid the high reflectivity stop gaps which would be encountered by the pump beam if it were also incident along the Γ-*M* direction. The region of pump-probe interaction is defined by the spot size and effective penetration depth of the probe beam, which is only a few photonic crystal unit cells.[11]

III. THEORETICAL CONCEPTS

For the pump beam incident along the pore axis, the dispersion curves are well known from work in PC fibers:[15] the mode frequency increases monotonically with wave number. The excited modes at 1.76 and 2.0 μm propagate with group velocity $v_u = 0.31c$ and $0.33c$, respectively, similar to that in bulk silicon and consistent with the fact that the field is concentrated in the silicon backbone. Although one might expect the respective field distributions to be confined but inhomogeneous in the silicon backbone, slight irregularities in the shape and size of the air pores along their axes may smear out the field distributions so that the latter can be treated as nearly uniform within the silicon backbone. Consequently, the effective pump intensity entering the PC is increased by a factor of $1/f$ (relative to the entering intensity) where $f = 0.42$ is the silicon filling fraction.

To clarify the optical effects that can tune the properties of silicon, consider the changes induced by a pump beam of frequency ω_p on the optical properties experienced by a probe beams of frequency ω_r. For any material in the dipole approximation, the optical susceptibility at frequency ω_r can be expanded in powers of the pump field; up to third order, the susceptibility takes the form[12]

$$\chi = \chi^{(1)}(\omega_r;\omega_r) + \chi^{(3)}(\omega_r;\omega_r,\omega_p,-\omega_p)E(\omega_p)E^*(\omega_p). \tag{1}$$

Because silicon is centrosymmetric, there is no second order response. Although the PC is anisotropic, for fixed polarization of pump and probe beams, we have ignored tensor considerations. The linear susceptibility $\chi^{(1)}$ defines the refractive index n_0 and linear absorption coefficient. For our pump and probe wavelengths, which correspond to photon energies below the indirect gap, linear absorption is absent. However, for wavelengths shorter than 2.2 μm, it is possible that 2PA (related to Im $\chi^{(3)}$) can occur and indeed, as seen below, is observable for high pump intensities. Since phonon participation is required for an indirect gap transition, it is not surprising that this absorption is weak and decreases rapidly with increasing wavelength. There is little data on 2PA in the pump wavelength region of interest to us although Dinu *et al.*[13] has recently given a value for the 2PA coefficient $\beta \sim 0.8$ cm/GW at 1.54 μm and 1.27 μm. For a 2PA process, the rate of carrier density (N) generation at a depth z [following the coordinate system indicated in Fig. 1(a)] in the sample is

$$\frac{\partial N(z,t)}{\partial t} = \frac{\beta I^2(z,t)}{2\hbar\omega_p}, \tag{2}$$

where the pump intensity I varies as

$$I(z) = \frac{(1-R_u)I_0}{f + \beta z(1-R_u)I_0} \tag{3}$$

according to attenuation by 2PA. Here, R_u is the sample reflectivity and I_0 is the incident pump intensity in the silicon at $(x,y,z=0)$. For a Gaussian pulse of FWHM pulse-width τ_p, the carrier density *following* the pulse passage is

$$N(z) = \frac{\sqrt{\pi}\beta\tau_p}{4\hbar\omega_p\sqrt{\ln 2}} I^2(z). \tag{4}$$

From Eq. (1), changes in the refractive index can be written as

$$\Delta n(\omega_r) = [\mathrm{Re}(\Delta\chi^{(1)}\ (\omega_r;\omega_r) + \chi^{(3)}(\omega_r;\omega_r,\omega_p,-\omega_p)E(\omega_p)E^*(\omega_p)]/2n_0 = \Delta n_0(\omega_r) + n_2(\omega_r,\omega_p)I. \tag{5}$$

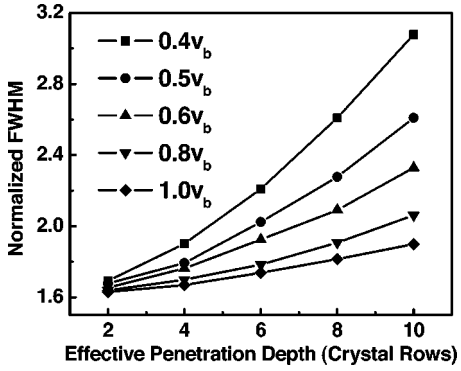

FIG. 2. Pump-probe interaction time in the PC (normalized to the convolution of the optical pulses in a collinear geometry in air) as a function of the effective probe penetration depth (measured in terms of crystal row separation in the Γ-*M* direction). The effective group velocity of the probe pulse in the PC is varied from 0.4 to 1 times that in bulk silicon.

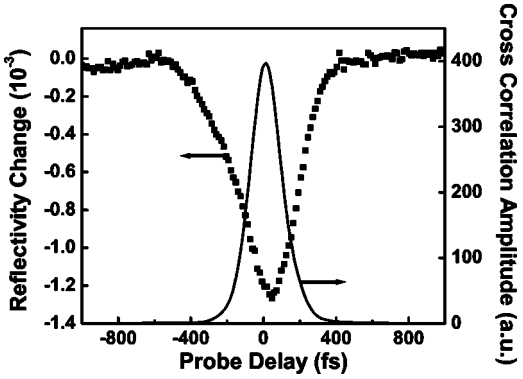

FIG. 3. Temporal response of reflectivity change at the 1.3 μm band edge when the PC is pumped with a 2.0 μm pulse at 17.6 GW/cm^2. Also shown is the cross correlation trace of the pump and probe pulses.

Changes in the linear refractive index $\Delta n_0(\omega_r)$ in principle can either be due to optically induced heating or the presence of injected carriers through the 2PA process. In the latter case, the so-called Drude contribution to the change in refractive index can be written as $\Delta n_0 = -Ne_2/2n_0\omega_r^2 m^* \varepsilon_0$, where m^* is the effective optical mass of the electrons and holes ($=0.16m_0$) and ε_0 is the permittivity of free space. For a peak pump intensity of 118 GW/cm^2, we estimate that the peak carrier density is 6×10^{17} cm^{-3} and Δn_0 is -1.2×10^{-3}.

The other contribution to the change in the refractive index $n_2(\omega_r, \omega_p)I$ is related to the nondegenerate Kerr effect which involves the virtual excitation of carriers in below band-gap transitions.[12] Values for these coefficients are not known although the degenerate n_2 has been determined recently[13,14] for Si(110) at 1.27 and 1.54 μm with values of 0.26×10^{-13} and 0.45×10^{-13} cm^2/W, respectively. Given that the wavelengths are far below the direct gap of silicon one does not expect significant dispersion in n_2 or differences between the nondegenerate and degenerate coefficients. Note that Kerr effect changes are instantaneous whereas Drude induced effects are not. However one can also distinguish the two contributions since the Kerr effect has a linear dependence on I whereas Drude effects vary as I^2. In the absence of significant absorption effects, one expects $\Delta R/R$ to be proportional to Δn for small changes.

For small changes in probe reflectivity (ΔR) induced by an optical Kerr effect with coefficient n_2 in the PC, one then has

$$\Delta R = \frac{dR}{d\lambda}\frac{d\lambda}{dn} n_2 I(z) \tag{6}$$

which becomes

$$\Delta R = \frac{dR}{d\lambda}\frac{d\lambda}{dn} n_2 \frac{1-R_u}{f} I_0 \tag{7}$$

in the limit of negligible 2PA. Here, $dR/d\lambda$ is the steepness of the band-edge reflectivity measured at the probe wavelength and $d\lambda/dn$ is the differential change in band-edge wavelength with refractive index. Similarly, the reflectivity change due to the Drude effect is given by

$$\Delta R = \frac{dR}{d\lambda}\frac{d\lambda}{dn}\frac{e^2}{2n_0\omega_r^2 m^* \varepsilon_0}\frac{\sqrt{\pi}\beta\tau_p}{4\hbar\omega_p\sqrt{\ln 2}} I^2(z). \tag{8}$$

Another way in which the PC influences the time-resolved reflectivity experiment relates to the interaction between pump and probe beams in the sample.[16] In particular the effective penetration depth of the probe beam is different than that of a bulk sample. For a probe penetration depth p, group velocity v_r, and spot size d, the convolution of the pump and reflected probe Gaussian pulses [following the coordinate system indicated in Fig. 1(a)] is proportional to

$$\int_{-d/2}^{d/2}\int_{-p}^{0}\int_{-\infty}^{0} \exp\{-a[(b-t)^2+(c-t)^2]\}dt\,dx\,dz + \int_{-d/2}^{d/2}\int_{0}^{p}\int_{0}^{\infty} \exp\{-a[(b-t)^2+(c-t)^2]\}dt\,dx\,dz, \tag{9}$$

where $a=4\ln 2/\tau_p{}^2$, $b=z/v_u+\tau_d$, and $c=x/v_r$. Here, τ_d is the relative delay between the pump and probe pulses. Figure 2 shows the results one obtains after numerically solving Eq. (9). For a given group velocity, long effective penetration depths for the probe pulse in the PC can lead to broadening of the time-resolved reflectivity traces relative to the optical

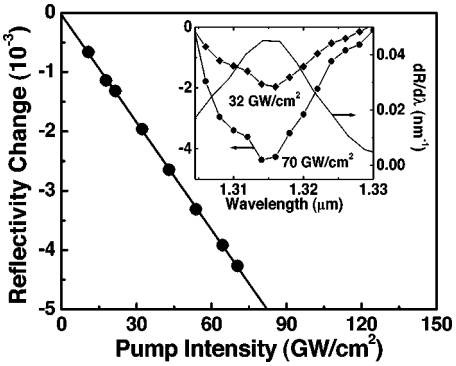

FIG. 4. Dependence of probe reflectivity change at 1.316 μm on pump intensity at zero delay. The inset shows the spectral characteristic of reflectivity change at the 1.3 μm band-edge at zero delay for different pump intensities at 2.0 μm. Also shown in the inset is the $dR/d\lambda$ curve which measures the steepness of the band-edge reflectivity.

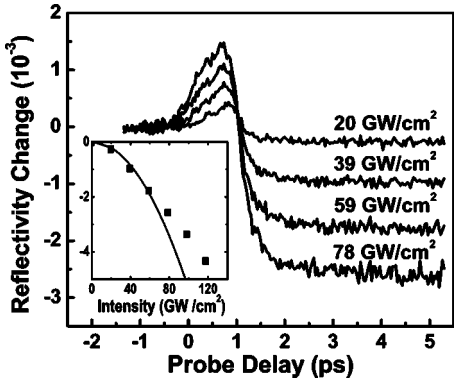

FIG. 5. Temporal response of the reflectivity change at the 1.6 μm band edge for different pump intensities at 1.76 μm. The inset shows the dependence of the carrier-induced reflectivity change on pump intensity for low pump powers.

pulse convolutions in air. The same effect is also obtained if the probe pulse propagates in the PC with an effective group velocity much slower than that in bulk silicon.

IV. EXPERIMENTAL RESULTS AND DISCUSSION

A. Kerr-induced changes induced by 2.0 μm pulses

Figure 3 shows the time dependent change in reflectivity at 1.3 μm for a 2.0 μm pump pulse and the cross-correlation trace of both pulses. The pump and probe intensities are 17.6 and 0.5 GW/cm^2, respectively. The decrease in reflectivity is consistent with a redshift of the band edge due to a positive nondegenerate Kerr index. The FWHM of the reflectivity trace is 365 ± 10 fs which is $1.8\times$ larger than the pump-probe cross-correlation width as measured by sum frequency generation in a BBO crystal. This difference can be explained in terms of pump and probe beam transit time effects in the PC as discussed above. Indeed, from the pump group velocity and probe spot size, one can deduce from Fig. 2 that the reflected probe pulse is delayed by 110 fs within the PC sample. After these effects are taken into account, the intrinsic interaction times are essentially pulse width limited, consistent with the Kerr effect.

One can use Eq. (7) to estimate a value for the nondegenerate Kerr coefficient in the silicon PC. Because of the relatively large values of $dR/d\lambda = 0.04\ \mathrm{nm}^{-1}$ and $d\lambda/dn = 174$ nm, induced reflectivity changes in the vicinity of the 1.3 μm band edge are found to be 70 times more sensitive than that in bulk materials for the same refractive index change, a degree of leverage also noted by others.[6,7] Indeed, when the PC is replaced by bulk crystalline silicon, *no change* in reflectivity is observed for our range of pump intensity. The inset to Fig. 4 shows there is good correlation between the change in probe reflectivity and the steepness of the band-edge reflectivity (measured separately) at different wavelengths and for a range of pump intensities. Figure 4 shows the change in reflectivity with pump intensity at zero time delay. The linear dependence is consistent with the Kerr effect and the nondegenerate Kerr index is estimated to be 5.2×10^{-15} cm^2/W. This is within an order of magnitude of the degenerate Kerr index reported[13,14] at 1.27 and 1.54 μm and represents reasonable agreement considering uncertainty in the lateral position (x) of the pump pulse in and its intensity at the probe location. It should also be noted that linear scattering losses as the pump pulse propagates through the PC along the pore axis have not been taken into account.

B. Kerr and plasma induced changes induced by 1.76 μm pulses

Results from experiments used to probe the 1.6 μm band edge when the sample is pumped with 1.76 μm pulses are illustrated in Fig. 5 which shows the temporal response of the change in probe reflectivity at different pump intensities for a probe intensity of 0.13 GW/cm^2. There is an initial increase and decrease in probe reflectivity on a subpicosecond time scale followed by a response that decays on a time scale of 900 ps and partially masks the Kerr effect near zero delay. At this band edge, the subpicosecond behavior is consistent with a Kerr effect similar to the previous experiments. The long time response could possibly be due to thermal or Drude contributions to the dielectric constant due to the generation of free carriers. Using a peak pump intensity of 120 GW/cm^2 and a 0.8 cm/GW 2PA coefficient[13,14] for 1.55 μm as an upper limit, one can estimate the surface peak carrier density to be $<10^{19}$ cm^{-3} and the maximum change in temperature to be <0.15 K. From the thermo-optic coefficient $\partial n/\partial T \sim 1\times10^{-4}$ K^{-1} at the probe wavelength,[17] the change in silicon refractive index is on the order of 10^{-5} and the (positive) induced change in reflectivity is expected to be about the same. From free carrier (Drude) contributions to the refractive index at our probe wavelength, changes to the imaginary part of the dielectric constant are about 2 orders of magnitude smaller than that of the real part[18] which is $\sim -10^{-3}$. Hence free carrier absorption of the probe pulse as well as thermally induced changes can be neglected in what follows and the change in reflectivity is ascribed to changes in the real part of the dielectric constant due to Drude effects.

At low pump powers the change in probe reflectivity scales quadratically with pump intensity, consistent with free

carrier generation by 2PA as given by Eq. (4). However, at higher pump intensities, consistent with Eq. (3), there is an apparent deviation from this quadratic dependence due to pump saturation effects as the inset in Fig. 5 shows. With increasing intensity in a 2PA process, an increasing fraction of the carriers are created closer to the surface where the pump pulse enters and the probe region develops a reduced and increasingly nonuniform carrier density. We estimate that at a depth of 60 μm, the expected saturation pump intensity is about an order of magnitude larger than the maximum pump intensity used here. The carrier lifetime of 900 ps is most likely associated with surface recombination within the PC sample with its large internal surface area.

From the low intensity behavior in the inset to Fig. 5, the 2PA coefficient, β, is estimated using Eq. (8) to be 0.02 cm/GW which is within an order of magnitude but smaller than that reported[12,13] for wavelengths near 1.55 μm. For the 2 μm pump wavelength, we estimate that the upper limit for β is 2×10^{-3} cm/GW, given our signal to noise and the fact that we observe no measurable long-lived response at the highest pump intensity used. This value is an order of magnitude smaller than what is determined at 1.76 μm and it is not a surprise since β is expected to decrease rapidly with increasing wavelength as the indirect gap edge is approached.

V. CONCLUSIONS

We have demonstrated how the real (Kerr) and imaginary (two-photon absorption) parts of a third order optical nonlinearity can be used to tune both band edges of a stopgap in a 2D silicon PC. At the short wavelength band edge, a 2 μm pump beam is used to demonstrate optical tuning via the Kerr effect, free from any nonlinear absorption. When the pump wavelength is changed to 1.76 μm for the 1.6 μm probe at the long wavelength edge, competition between the Kerr and Drude effects is observed. The former causes a nearly pulse-width limited redshift in the band edge; the latter causes a blueshift in the band edge, which lasts for the carrier recombination time.

ACKNOWLEDGMENTS

H.W.T. and H.vD. gratefully acknowledge the financial support of Photonics Research Ontario and the Natural Sciences and Engineering Research Council. R.B.W. thanks the DFG in the SPP 113 under WE 2637/3. The authors also thank J. Sipe and S. Volkov for useful discussions.

[1] K. Yoshino, S. Satoh, Y. Shimoda, Y. Kawagashi, K. Nakayama, and M. Ozaki, Jpn. J. Appl. Phys., Part 2 **38**, L961 (1999).
[2] S. W. Leonard, J. P. Mondia, H. M. van Driel, O. Toader, S. John, K. Busch, A. Birner, U. Gosele, and V. Lehmann, Phys. Rev. B **61**, R2389 (2000).
[3] D. Kang, J. E. Maclennan, N. A. Clark, A. A. Zakhidov, and R. H. Baughman, Phys. Rev. Lett. **86**, 4052 (2001).
[4] A. Hache and M. Bourgeois, Appl. Phys. Lett. **77**, 4089 (2000).
[5] X. Hu, Q. Zhang, Y. Liu, B. Cheng, and D. Zhang, Appl. Phys. Lett. **83**, 2518 (2003).
[6] S. W. Leonard, H. M. van Driel, J. Schilling, and R. B. Wehrspohn, Phys. Rev. B **66**, 161102 (2002).
[7] A. D. Bristow, W. H. Fan, A. M. Fox, M. S. Skolnick, D. M. Whittaker, A. Tahraomi, T. F. Krauss, and J. S. Roberts, Appl. Phys. Lett. **83**, 851 (2003).
[8] P. M. Johnson, A. F. Koenderink, and W. L. Vos, Phys. Rev. B **66**, 081102 (2002).
[9] M. Shimizu and T. Ishihara, Appl. Phys. Lett. **80**, 2836 (2002).
[10] J. M. Fraser and H. M. van Driel, Phys. Rev. B **68**, 085208 (2003).
[11] S. W. Leonard, H. M. van Driel, K. Busch, S. John, A. Birner, A.-P. Li, F. Muller, U. Gosele, and V. Lehmann, Appl. Phys. Lett. **75**, 3063 (1999).
[12] R. W. Boyd, *Nonlinear Optics* (Academic, San Diego, 2003), p. 190.
[13] M. Dinu, F. Quochi, and H. Garcia, Appl. Phys. Lett. **82**, 2954 (2003).
[14] H. K. Tsang, C. S. Wong, T. K. Liang, I. E. Day, S. W. Roberts, A. Harpin, J. Drake, and M. Asghari, Appl. Phys. Lett. **80**, 416 (2002).
[15] J. C. Knight, T. A. Birks, P. St.J. Russell, and J. P. de Sandro, J. Opt. Soc. Am. A **15**, 748 (1998).
[16] J. C. Diels and W. Rudolph, *Ultrashort Laser Pulse Phenomena* (Academic, London, 1996), p. 404.
[17] *Landolt-Bornstein 17-a*, edited by K.-H. Hellwege (Springer, Berlin, 1982), p. 70.
[18] M. I. Gallant and H. M. van Driel, Phys. Rev. B **26**, 2133 (1982).